X-ray reflection spectra from ionized slabs

R. R. Ross,[1] A. C. Fabian[2]★ and A. J. Young[2]

[1]*Physics Department, College of the Holy Cross, Worcester, MA 01610, USA*
[2]*Institute of Astronomy, Madingley Road, Cambridge CB3 0HA*

ABSTRACT

X-ray reflection spectra are an important component in the X-ray spectra of many active galactic nuclei and Galactic black hole candidates. It is likely that reflection takes place from highly ionized surfaces of the accretion disc in some cases. This can lead to strong Comptonization of the emergent iron, and other absorption and emission features. We present such reflection spectra here, computed in a self-consistent manner with the method described by Ross & Fabian. In particular we emphasize the range where the ionization parameter (the flux to density ratio) ξ is around and above 10^4. Such spectra may be relevant to the observed spectral features found in black hole candidates such as Cygnus X-1 in the low/hard state.

Key words: accretion, accretion discs – line: profiles – radiative transfer – galaxies: active – X-rays: general – X-rays: stars.

1 INTRODUCTION

Compton reflection is an important component of the X-ray spectrum of many compact objects (Guilbert & Rees 1988; Lightman & White 1988), particularly of active galactic nuclei (AGN) and black hole candidate (BHC) sources. It is produced when the primary X-ray emission from the source strikes Thomson-thick matter, which Compton scatters X-rays into our line of sight. In many cases the accretion flow, probably a disc, is the major scattering medium. If that matter were solely composed of hydrogen then the reflection continuum would have the same spectral shape as the primary emission in the X-ray band, decreasing above about 30 keV owing to Compton recoil. Other elements such as oxygen and iron, if they are not highly ionized, can absorb the lower energy X-rays and so flatten the reflection continuum and, in particular in the case of iron, add fluorescent line emission (George & Fabian 1991; Matt, Perola & Piro 1991). Measurements of the strength and shape of the reflection spectrum can yield the geometry, velocity, gravitational potential depth and abundances of the scattering medium.

As the X-ray irradiation of the medium becomes more intense, so the matter becomes ionized. This reduces the effects of absorption, progressively from lower to higher energies as the intensity increases (Lightman & White 1988; Done et al. 1992; Ross & Fabian 1993; Życki et al. 1994). An important signature of ionized reflection is a strong iron edge. Iron is a strong absorber when the gas is neutral, but absorption both above and below the edge are so strong that the change in observed flux across the edge is small, particularly if the primary continuum is also observed. When much of the oxygen in the gas is completely ionized the edge appears

much stronger because the absorption below it is reduced. Of course, the energy of the iron emission line shifts up in energy from 6.4 through 6.7 to 6.97 keV as iron is ionized, but Doppler shifts may confuse precise estimates of the observed energy. The line can be weak when iron is ionized to Fe XVII–Fe XXIII as line photons can be resonantly scattered and destroyed by Auger events (Ross, Fabian & Brandt 1996). Moreover, as the fraction of completely stripped iron increases, the line may be significantly broadened by Comptonization and so become less apparent in the observed spectrum (Matt, Fabian & Ross 1996). Relativistic blurring when the reflection is from an accretion disc can further merge the line and edge so that neither is distinct in the final spectrum. The net result can be a weak broad absorption trough that starts at about 7 keV.

Unlike the reflection spectrum from relatively neutral gas, which depends mainly upon the relative abundance of the elements and can be computed in a straightforward manner by the Monte Carlo technique, the spectrum when the gas is partially ionized requires detailed numerical calculation to obtain the temperature, ionization structure and resultant Comptonization (Ross 1979). We have previously computed examples appropriate for simple accretion discs around AGN and BHC, concentrating mainly on ionization parameters $\xi = 4\pi F/r^2 \lesssim 10^3$ where Auger destruction can be important (Ross & Fabian 1993). However as the precise density structure of the outer few Thomson depths of an accretion disc where the reflection spectrum is formed is unknown (the total disc thickness may be hundreds of Thomson depths), we consider a wider range of conditions here and highlight the range at higher values of $\xi \sim 10^4$, the details of which have been largely ignored in previous work.

This range of ξ may be particularly relevant to the spectra of many BHC in the low/hard state, which show only a small reflection

★E-mail: acf@ast.cam.ac.uk

component (Ebisawa 1991; Ebisawa et al. 1994, 1996; Gierliński et al. 1997; Życki, Done & Smith 1998; Done & Życki 1998). One popular interpretation for this is that the central parts of the disc out to 30–50 gravitational radii are missing and replaced by a hot cloud, which gives no intrinsic reflection (Gierliński et al. 1997; Życki et al. 1998; Poutanen 1998). What reflection is seen comes from the outer disc. We point out the alternative that, in a geometry where the primary X-rays are produced above a disc, an apparent lack of reflection could indicate high reflection. In principle, there is no difference in the spectrum expected from a single hot cloud and one with a perfect mirror bisecting it. In practice, Compton reflection is not perfect, but departures from a uniform albedo can be small in the 1–30 keV range where most spectral fitting takes place. We show here that the small departures from uniformity owing to iron features that occur in a highly ionized disc can account for the small reflection signature seen, without the need to illuminate the outer disc. This solution may also be relevant to the X-ray spectra of many quasars, which also show little evidence for reflection yet are generally assumed to be powered by disc accretion (Nandra et al. 1995, 1997).

We note that values of $\xi \sim 10^4$ appear to imply an accretion rate close to the Eddington limit for a standard accretion disc [Ross & Fabian (1993) show that $\xi = 7 \times 10^4 f^3$, where f is the Eddington ratio]. However, if there is a patchy corona above the disc (see e.g. Stern et al. 1995), rather than a continuous one, with a covering fraction of f_A then $\xi > 10^4$ requires $f > f_A/7$, which is only a per cent or so when $f_A \sim 0.1$. Moreover, these estimates assume a uniform density for the disc right to its surface. The outer few Thomson depths could well have a lower density and thus mean that ξ is underestimated.

In this paper, we present and discuss detailed, self-consistent computations of the temperature and ionization structure of slabs of gas ionized by the incident radiation and of the resulting reflection spectra. We assume both a constant density for the gas and a Gaussian fall off. The spectra will be compared with X-ray observations of BHC in future work.

2 COMPUTATIONS

2.1 Method

We consider a slab of gas the surface of which is illuminated by radiation with a power-law spectrum of photon index Γ. The radiative transfer is calculated for the upper layer of the slab that is responsible for producing the reflected spectrum. In order to concentrate solely on the effects of the illumination, no radiation is taken to enter the treated layer from the remainder of the slab beneath it.

The method used has been described in detail by Ross & Fabian (1993). The illuminating radiation is treated analytically in a 'one-stream' approximation. The diffuse radiation that results from Compton scattering of the incident radiation and from emission within the gas is treated using the Fokker–Planck/diffusion method of Ross, Weaver & McCray (1978) modified for plane-parallel geometry. The local temperature and ionization state of the gas is found by solving the equations for thermal and ionization equilibrium, so that they are consistent with the local radiation field. Hydrogen and helium are assumed to be fully ionized, while the following ionization stages of the most abundant metals are treated: C v–vii, O v–ix, Mg ix–xiii, Si xi–xv, and Fe xvi–xxvii.

For a given value of Γ, the temperature and ionization state of the outer portion of the slab is expected to depend primarily on the value of the ionization parameter,

$$\xi = \frac{4\pi F}{n_H}, \tag{1}$$

where F is the total illuminating flux (from 0.01–100 keV) and n_H is the hydrogen number density. For uniform-density slabs, we vary ξ by changing the total illuminating flux while keeping the hydrogen number density fixed at $n_0 = 10^{15}\ \mathrm{cm}^{-3}$. This is a typical density that might be found in an AGN accretion disc. At the higher density expected for a BHC accretion disc, the effects of three-body recombination and heating owing to free–free absorption cause the temperature and ionization state to depend somewhat on n_H as well as ξ (e.g., see Ross 1979). However, this should have very little effect on the X-ray spectral features resulting from iron, which should remain similar to those calculated here.

2.2 Results

Fig. 1 shows the results for a uniform slab illuminated by a $\Gamma = 2$ spectrum with an ionization parameter $\xi = 10^4$. The illuminating and reflected spectra are displayed as EF_E versus E, where E is the photon energy and F_E is the spectral energy flux. The slab is highly reflecting, with $F_E(\mathrm{out})/F_E(\mathrm{in}) > 63$ per cent throughout the 2–20 keV spectral band. This is because the gas is highly ionized. At the illuminated surface, the iron is 85 per cent fully ionized, 14 per cent Fe xxvi, and 1 per cent Fe xxv. The Fe xxvi fraction peaks at 45 per cent around Thomson depth $\tau_T \sim 2.5$. Fe xxv is the dominant ion for $3.5 \lesssim \tau_T \lesssim 7.5$. Silicon and magnesium (not shown in Fig. 1) are fully ionized throughout the regions where Fe xxv–xxvii dominate. For $\tau_T \gtrsim 10$, iron ions have all their L-shell electrons, while magnesium and silicon ions have filled K-shells.

Despite the high ionization of the surface layers, the reflected spectrum shows features owing to iron Kα emission and K-shell absorption. Most of the Kα photons emerge in a broad Comptonized emission feature that blends smoothly into the Compton-smeared absorption feature. Only a small fraction of the Kα photons emerge in narrow Fe xxv and Fe xxvi line cores at 6.7 and 7.0 keV, respectively; these are shown in Fig. 1 with a spectral resolution $\delta E/E \approx 2$ per cent. Fe xxvi Kα photons are subject to resonance trapping. Many are removed from the narrow-line core by an initial Compton scattering and then are further Comptonized as they diffuse outward to the surface. The Fe xxv intercombination line is not subject to resonance trapping, but most of these photons are produced at such great depth that they also suffer repeated Compton scatterings before escaping. To clarify the contribution of the Comptonized line, Fig. 1 also shows the reflected spectrum when the iron Kα emission is artificially suppressed. The Kα photons form an important part of the reflected continuum for $4 \lesssim E \lesssim 9$ keV. Also shown in Fig. 1 is the reflected spectrum if all iron features are suppressed by setting the iron abundance to zero. Relative to this smooth spectrum, the actual reflection spectrum is enhanced for $E < 7.5$ keV and depleted for $E > 7.5$ keV

For soft X-rays ($E \lesssim 1.5$ keV in this case) not shown in Fig. 1, the emergent spectral flux exceeds the incident flux owing to bremsstrahlung emission by the hot surface layers and 'inverse Compton' upscattering of even softer photons. The *total* flux leaving the surface over the entire spectral range under consideration ($0.01\,\mathrm{keV} \leq E \leq 100\,\mathrm{keV}$) equals the total incident flux, as required by the condition of thermal equilibrium. The reflected spectrum declines steeply above ~ 50 keV because of the sharp cut-off assumed at 100 keV. Extending the illuminating spectrum to higher energies (with an exponential cut-off, say) would raise this
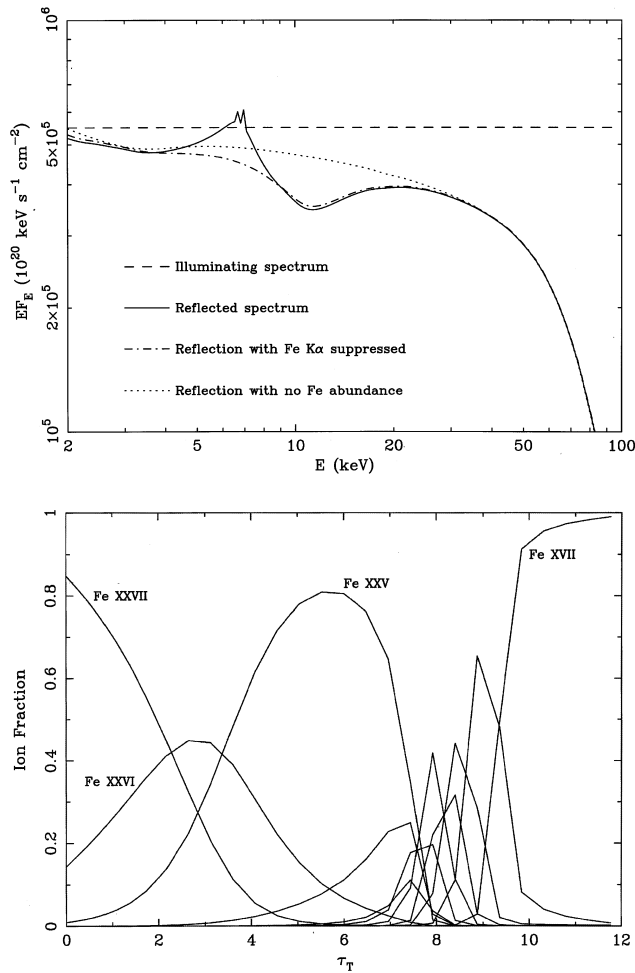
Figure 1. Illumination of a uniform slab with $\Gamma = 2$ and $\xi = 10^4$. Top panel: reflected spectrum. Bottom panel: iron ion fractions versus Thomson depth.
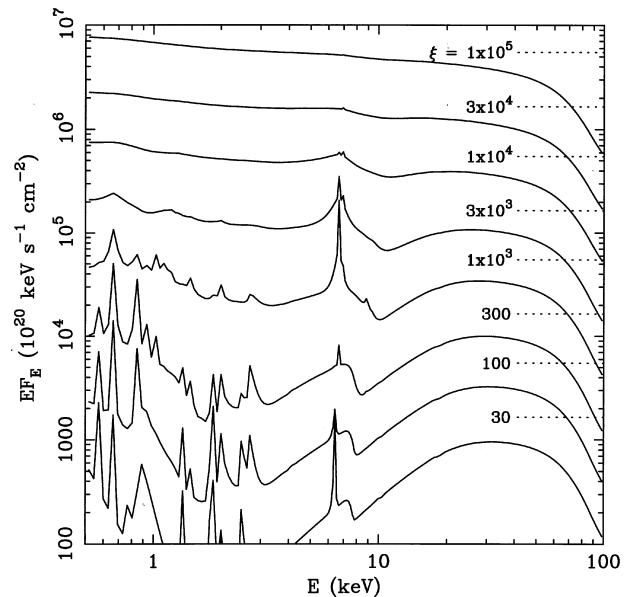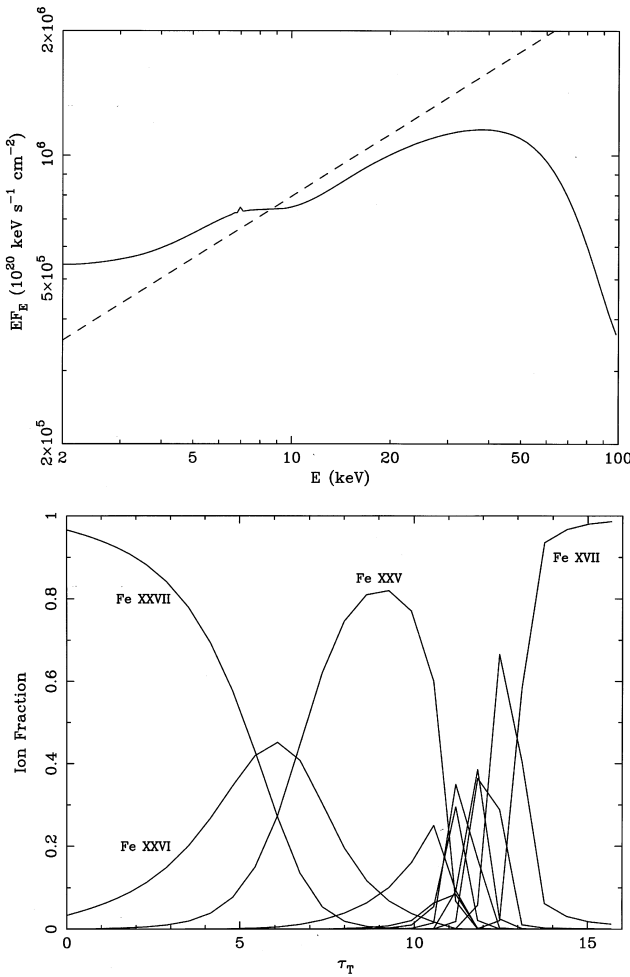

Figure 2. Reflection spectra for illumination of a uniform slab with $\Gamma = 2$ and various values of the ionization parameter. The number above each curve indicates the corresponding ξ value, and the dotted line to the right of that number indicates the constant value of EF_E for that illumination.

portion of the emergent spectrum via Compton downscattering of higher energy photons, but would have little effect on the iron ionization structure and spectral features.

The temperature at the illuminated surface is found to be 1.5×10^7 K. In the highly ionized gas there, heating owing to Compton downscattering of hard photons dominates over heating owing to photoabsorption. Therefore, the temperature should not exceed the 'Compton temperature', T_C, at which Compton heating would be balanced solely by cooling owing to 'inverse Compton' upscattering of soft photons. This condition is given by

$$4kT_C \int_{E_1}^{E_2} u_E \, dE = \int_{E_1}^{E_2} u_E \left(E - \frac{21E^2}{5m_e c^2} \right) dE, \quad (2)$$

where u_E is the spectral energy density of the radiation, while E_1 and E_2 are the lower and upper limits, respectively, of the spectrum under consideration. The right-hand side of this equation includes the reduction in Compton heating owing to first-order Klein–Nishina corrections to the scattering cross-section (see Ross 1979). Setting $u_E \propto E^{1-\Gamma}$ for the illuminating radiation, this gives $T_C = 1.9 \times 10^7$ K for $\Gamma = 2$. The temperature that we find at the surface is slightly lower than the Compton temperature owing to additional cooling by bremsstrahlung emission.

This disagrees with the results of Życki et al. (1994), who found a surface temperature exceeding 4×10^7 K for illumination with

$\xi = 10^4$ by a spectrum that was only slightly flatter ($\Gamma = 1.9$). The Monte Carlo calculation of Życki et al. only treated photons in the range $0.15 \, \text{keV} \leq E \leq 100 \, \text{keV}$ and did not include the thermal emission by the gas itself. This leads to underestimation of the inverse Compton cooling rate and thus to the high surface temperature (and the steep temperature gradient) that they found.

Fig. 2 shows a series of reflection spectra under similar conditions with ionization parameters ranging from $\xi = 30$ to 10^5. The model with the highest ionization parameter, $\xi = 10^5$, is an excellent reflector and exhibits negligibly small spectral features resulting from iron. This is because the surface layer is fully ionized to great depth, with Fe XXVI not becoming dominant until $\tau_T \approx 8$. The Compton reflection produces a slight steepening in the reflected spectrum compared with the illumination; the reflected component mimics a power law with $\Gamma = 2.14$ in the 2–20 keV band. The temperature at the illuminated surface is found to be 1.9×10^7 K, the full Compton temperature for a $\Gamma = 2$ power-law spectrum.

When the illuminating flux is reduced so that $\xi = 3 \times 10^4$, the Kα emission and K-shell absorption features resulting from iron begin to become apparent. Fully-ionized iron dominates for $\tau_T \lesssim 5$, so the emission and absorption features are weak and are highly broadened by Compton scattering. When ξ is reduced to 10^4, the broad spectral features resulting from iron become more important. This model has already been discussed in detail.

With ξ reduced to 3×10^3, less than half of the iron is fully ionized at the illuminated surface, and Fe XXV becomes dominant at $\tau_T \approx 1$. Now an important *narrow* emission line resulting from Fe XXV can be seen in addition to a Compton-broadened emission feature in Fig. 2. This is primarily owing to emission of the intercombination line following recombination to excited states. When ξ is further reduced to 10^3, Fe XXV dominates at the illuminated surface, and the narrow Fe XXV Kα line is quite strong. The tiny emission feature just above 8.8 keV is the result of radiative recombination directly to the ground level of Fe XXV. Similarly, Si XIV produces two emission features: one at 2.01 keV resulting from Kα emission and the other just above 2.67 keV

Figure 3. Illumination of a uniform slab with $\xi = 10^4$ for a $\Gamma = 1.5$ power law. Top panel: reflected spectrum (solid curve) and illumination (dashed line). Bottom panel: iron ion fractions versus Thomson depth.

resulting from radiative recombination. (See Życki et al. 1994 for other examples of radiative recombination emission features.) The exact strength of these and other low-energy spectral features could be affected by absorption by elements such as nitrogen and neon, which we do not include in our calculations, and we do not calculate the features owing to sulphur.

The narrow Fe Kα emission line is suppressed in the models with $\xi = 300$ and $\xi = 100$. This is because ions in the range Fe XVII–Fe XXIII dominate at the illuminated surface, and their Kα photons are assumed to be destroyed by the Auger effect during resonance trapping (see Ross & Fabian 1993; Życki & Czerny 1994; Ross et al. 1996). The narrow line seen when $\xi = 300$ is the result of a small amount of Fe XXV near the surface. On the other hand, the narrow line seen when $\xi = 100$ is the result of Fe XVI, the least ionized species that we treat, which then dominates for $\tau_T \gtrsim 0.5$. Finally, for $\xi = 30$ the reflection is similar to that of a cold, neutral slab, and the narrow emission line at 6.4 keV is strong.

The ionization structure in the outer layers of the illuminated slab depends on the spectral form of the illumination as well as on the ratio of total flux to gas density expressed by the parameter ξ. Fig. 3 shows the results with $\xi = 10^4$ again, but when the illuminating spectrum is a flatter power law with $\Gamma = 1.5$. Now a greater fraction of the illuminating photons lie in the 9–20 keV range that is
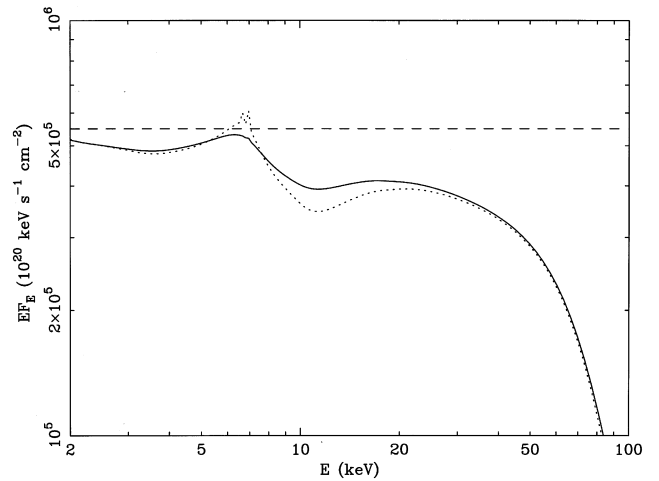
Figure 4. Illumination with $\Gamma = 2$ and $\xi_0 = 10^4$ when there is a Gaussian drop-off in density at the top of the slab with a Thomson depth $\tau_T = 5$. The reflected spectrum and the incident illumination are shown by the solid and dashed curves, respectively. Also shown for comparison is the reflected spectrum (dotted curve) for uniform density from Fig. 1.

so important in producing fully photoionized iron. As a result, Fe XXVII dominates to greater depth ($\tau_T \lesssim 5.5$) than when $\Gamma = 2$, and the Compton-broadened emission and absorption features owing to iron are not as strong.

One of the uncertainties in modelling Compton reflection is the density structure of the illuminated gas. In the models presented above, the gas density has been assumed to be uniform with depth. This is the case, for example, in the standard Shakura & Sunyaev (1973) theory of accretion discs (also see Laor & Netzer 1989). However, this probably is not realistic even for a bare accretion disc (e.g., see Shakura, Sunyaev & Zilitinkevich 1978; Shimura & Takahara 1993), and it certainly cannot be the case when the surface has strong external illumination. The heating of the outermost layers by the impinging radiation should result in a decrease in density there.

In order to see the general effect of such a decrease in density, let us arbitrarily assume that a constant-density slab (with $n_H = n_0$) is topped by a 'boundary layer' in which the density decreases with height in a Gaussian manner,

$$n_H(z) = n_0 \exp\left(-\frac{z^2}{h^2}\right). \tag{3}$$

Here z is the height above the base of the boundary layer, and h is its characteristic thickness. As the illuminating radiation is expected to have an important effect down to a Thomson depth of a few, we let the boundary layer have a total Thomson depth

$$\tau_T = 1.2 n_0 \sigma_T h \frac{\sqrt{\pi}}{2} = 5, \tag{4}$$

where the free electron density is assumed to be $n_e = 1.2 n_H$. Fig. 4 shows the result when such a gas is illuminated by a $\Gamma = 2$ power law with a flux that would yield an ionization parameter $\xi_0 = 4\pi F/n_0 = 10^4$ for gas at the base density. As the gas density is lower in the boundary layer, the effective ionization parameter is higher there. As a result, iron is 88 per cent fully ionized at Thomson depth $\tau_T = 1$, compared with only 69 per cent fully ionized for the uniform-density slab shown in Fig. 1. In fact, Fe XXVII dominates all the way down to $\tau_T \approx 3.5$. The broad, Comptonized, iron Kα emission and K-shell absorption features in the reflected spectrum
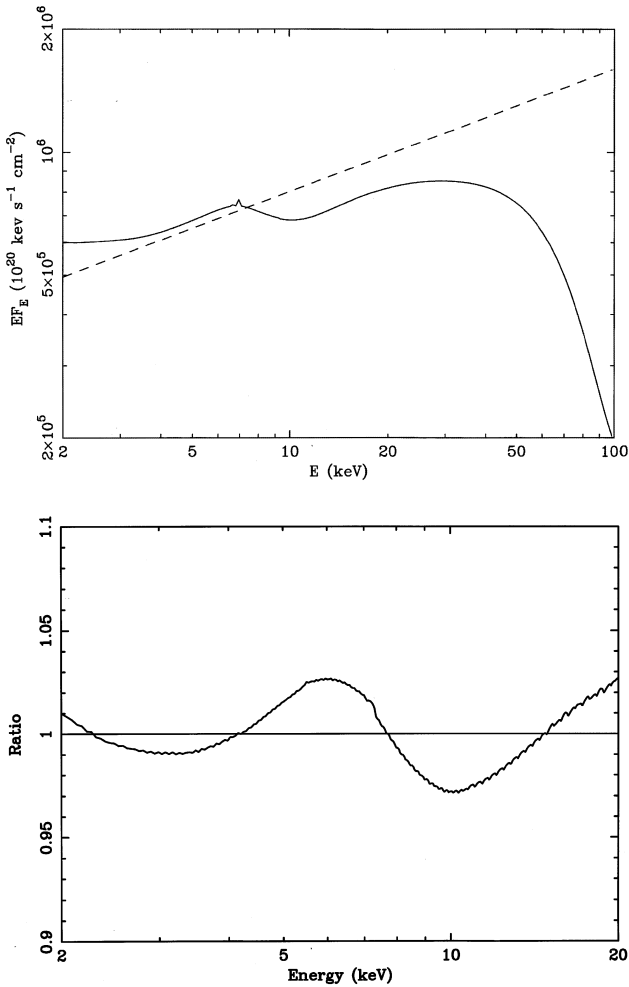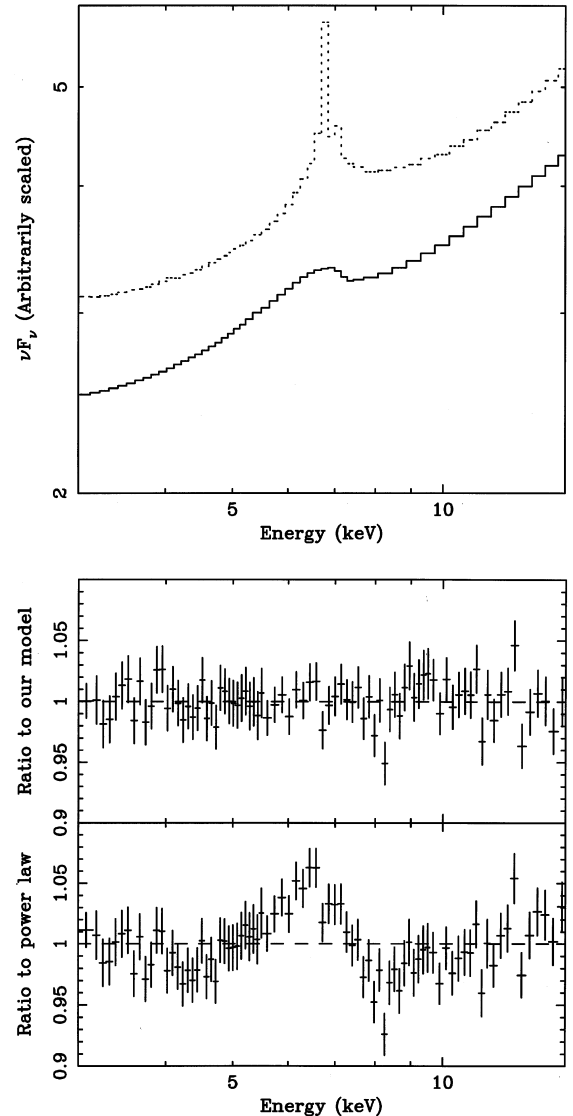
Figure 5. Illumination of a uniform slab with $\xi = 10^4$ for a $\Gamma = 1.7$ power law. Top panel: illumination (dashed line) and reflected spectrum (solid curve). Bottom panel: ratio of total spectrum (incident plus reflected) to best-fitting power-law model after taking into account smearing by relativistic effects for emission by an annulus at $7R_S$ around a black hole.

are not as strong as for the uniform-density slab. Of particular importance is the fact that the narrow Kα line cores, which were already weak in the uniform-density case, are now almost totally suppressed.

3 DISCUSSION

For X-ray illumination with $\xi \sim 10^4$ or higher, the features in the reflected spectrum owing to iron Kα emission and K-shell absorption are weak and are smeared out by Compton scattering. Any narrow Fe Kα line cores are extremely weak. These effects are further enhanced when the illuminating spectrum is harder (flatter) or when there is a drop-off in gas density owing to the heating by the external illumination.

Such effects may come into play in the formation of X-ray spectra of black hole candidates. In the past, *Ginga* spectra of BHCs have been interpreted as exhibiting broad iron absorption features ('smeared edges') with very weak Fe Kα lines (Ebisawa 1991; Tanaka 1991; Ebisawa et al. 1994). This led to the suggestion that the line is suppressed by resonant Auger destruction in Fe XVII–XXIII (Ross & Fabian 1993; Ueda, Ebisawa & Done 1994; Ross et al. 1996).

Figure 6. Illumination of uniform slab with $\xi = 7400$, $\Gamma = 1.5$ and twice solar iron abundance. Upper panel: unblurred (dotted line) and relativistically blurred (solid line) illuminating plus reflected spectra. Centre panel: ratio of data to our model (the blurred one from the upper panel). Lower panel: ratio of data to simple power law.

However, recent spectral studies of *Ginga*, *EXOSAT* and *ASCA* BHC in the low/hard state have found broad Fe Kα emission features as well as K-shell absorption features (Życki, Done & Smith 1997; Życki et al. 1998; Done & Życki 1998). These studies have treated the broadening of the features as being the result of relativistic smearing by the reflecting accretion disc. The ξ values derived for the illumination have been very low, and the weakness of the iron features has been taken to imply that the disc subtends a solid angle of illuminating radiation considerably smaller than 2π. [Done & Życki conclude that the broadening of the disc Kα line makes it difficult to detect with *ASCA*, so the narrow line found by Ebisawa et al. (1996) comes from the companion star.] This has led to the conclusion that the optically thick accretion disc only extends inward to a few tens of gravitational radii.

As an alternative, the broad and weak iron features could be the result of illumination of the disc with $\xi \gtrsim 10^4$. Fig. 5 shows the incident and reflected spectra for illumination with $\xi = 10^4$ and a
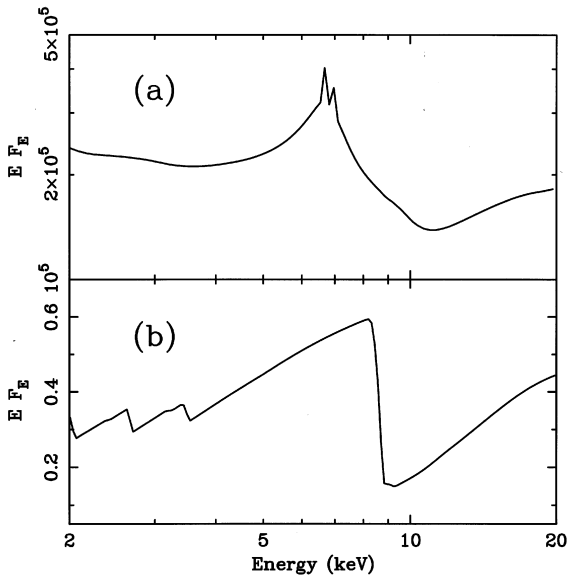
Figure 7. The reflection component from the present work for $\xi = 5000$ (a) and from the PEXRIV model (Magdziarz & Zdziarski 1995) in XSPEC with a corresponding $\xi = 4500$ (when the different energy range is corrected for) and disc temperature of 10^6 K (b). The PEXRIV spectrum is just for the continuum, whereas spectrum (a) includes the iron emission lines, the level of contribution of which can be assessed from Fig. 1. Note from our spectra shown here, and in Fig. 2, that we never obtain a strong edge dropping above 8 keV, as seen in the PEXRIV model.

power-law index $\Gamma = 1.7$. If the primary X-ray emission is from a corona immediately above the accretion disc, the reprocessor subtends a full $\Omega = 2\pi$, and the total observed spectrum is the sum of the illuminating flux (resulting from the half of the radiation emitted in the outward direction) and the reflected flux. Fig. 5 shows the result after relativistic smearing if this total flux is assumed to originate from a narrow annulus at radius $7R_S$ inclined at $30°$ around a Kerr black hole. Over the 2–20 keV range, the best-fitting power law now has a slope of $\Gamma = 1.79$. The ratio of the observed spectrum to the best-fitting power-law model shows broad emission and absorption features markedly similar to those found by Done & Życki (1998) for the *EXOSAT* spectrum of Cyg X-1. There are several features to note here: Comptonization of the edge means that it begins around 6 keV (dash–dot curve in Fig. 1) and now resembles more a symmetrical trough than a convential photoelectric absorption edge; the Comptonized and smeared line emission fills in the lower energy part of this trough so that the whole feature mimics an edge at about 7 keV.

Encouraged by the similarity bewteen our model and the observed spectra shown by Done & Życki (1998), we have fitted a grid of our models to the brightest of the archival *EXOSAT* spectra. The models are relativistically blurred using the Kerr metric kernel of Laor (1991). The best fit over the 3–15 keV range indicates $\xi = 7400$ and $\Gamma = 1.5$ for an iron abundance twice the solar value (Fig. 6, upper and centre panels) from a disc inclined at less than $30°$ and extending from $1.235\,m$ to $100\,m$, with surface emissivity varying as (radius)$^{-3}$. In the lower panel we show the ratio of the data to the best-fitting power-law model, which strongly resembles the similar plot by Done & Życki (1998) for all the *EXOSAT* data.

It is interesting to compare the result of our calculation with that given by the PEXRIV code (Magdziarz & Zdziarski 1995) in the XSPEC package for a value of $\xi = 5000$, which is within the range

allowed by that code (we correct for the different energy ranges used to define ξ in our codes). This is shown in Fig. 7. There is clearly a large difference, particularly in the position of the iron edge (the PEXRIV code does not predict the iron-line properties, which must be added separately). The PEXRIV code does not take account of the Comptonization of the features in the outer, most highly ionized layers. We advise against the use of this code for high values of ξ and for the use of our approach, or that of Życki et al. (1994; see also Böttcher, Liang & Smith 1998).

A detailed model for an ionized accretion disc will necessarily require a range of ξ to be present, both from different radii, and at different distances from the ionizing source if the corona is patchy. The results shown in this paper will be useful as a guide to situations dominated by highly ionized matter, for example where the size of separate patches of a corona exceed their height above the disc. We intend to pursue a detailed comparison with observed spectra in future work.

REFERENCES

Böttcher M., Liang E. P., Smith I. A., 1998, A&A, 339, 87
Done C., Mulchaey J. S., Mushotzky R. F., Arnaud K. A., 1992, ApJ, 395, 275
Done C., Życki P. T., 1998, preprint (astro-ph 9812261)
Ebisawa K., 1991, PhD thesis, Univ. Tokyo
Ebisawa K. et al., 1994, PASJ, 46, 375
Ebisawa K., Ueda Y., Inoue H., Tanaka Y., White N. E., 1996, ApJ, 467, 419
George I. M., Fabian A. C., 1991, MNRAS, 249, 352
Gierliński M., Zdziarski A. A., Done C., Johnson W. N., Ebisawa, K., Ueda Y., Haardt F., Phlips B. F., 1997, MNRAS 288, 958
Guilbert P. W., Rees M. J., 1988, MNRAS, 233, 475
Laor A., 1991, ApJ, 376, 90
Laor A., Netzer H., 1989, MNRAS, 238, 897
Lightman A. P., White T. R., 1988, ApJ, 335, 57
Magdziarz P., Zdziarski A. A., 1995, MNRAS, 273, 837
Matt G., Fabian A. C., Ross R. R., 1996, MNRAS, 278, 1111
Matt G., Perola G. C., Piro L., 1991, A&A, 247, 25
Nandra K., Fabian A. C., Brandt W. N., Kunieda H., Matsuoka M., Mihara T., Ogasaka Y., Terashima Y., 1995, MNRAS, 276, 1
Nandra K., George I. M., Mushotzky R. F., Turner T. J., Yaqoob T., 1997, ApJ, 488, L91
Poutanen J., 1998, preprint (astro-ph 9805025)
Ross R. R., 1979, ApJ, 233, 334
Ross R. R., Fabian A. C., 1993, MNRAS, 261, 74
Ross R. R., Fabian A. C., Brandt W. N., 1996, MNRAS, 278, 1082
Ross R. R., Weaver R., McCray R., 1978, ApJ, 219, 292
Shakura N. I., Sunyaev R. A., 1973, A&A, 24, 337
Stern B. E., Poutanen J., Svensson R., Sikora M., Begelman, M. C., 1995, ApJ, 449, L13
Tanaka Y., 1991, in Treves A., Perrola G. C., Stella L., eds, Lecture Notes in Physics 385, Iron Line Diagnostics in X-ray Sources. Springer, Berlin, p. 98
Ueda Y., Ebisawa K., Done C., 1994, PASJ, 46, 107
Życki P. T., Czerny, B., 1994, MNRAS, 266, 653
Życki P. T., Done C., Smith D. A., 1997, ApJ, 488, L113
Życki P. T., Done C., Smith D. A., 1998, ApJ, 496, L25
Życki P. T., Krolik J. H., Zdziarski A. A., Kallman T. R., 1994, ApJ, 437, 597

This paper has been typeset from a T$_E$X/L^{A}T$_E$X file prepared by the author.